Computational Study on Impurities Poisoning and Degradation of an SOFC Anode Based on Density Functional Theory

T. Ogura[a,b], K. Nakao[b], T. Ishimoto[a], and M. Koyama[a,b,c]

[a] INAMORI Frontier Research Center, Kyushu University, Fukuoka 819-0395, Japan
[b] Department of Hydrogen Energy Systems, Graduate School of Engineering
Kyushu University, Fukuoka 819-0395, Japan
[c] International Institute for Carbon-Neutral Energy Research (I[2]CNER)
Kyushu University, Fukuoka 819-0395, Japan

Solid oxide fuel cells (SOFCs) are expected to be the most efficient and versatile system for chemical to electrical energy conversion. One of advantages of SOFC is the possibility of direct utilization of various types of hydrocarbon fuels. It is however well known that fuel impurities in practical SOFC fuels such as sulfur compounds could cause SOFC poisoning or degradation. Therefore, understanding the effect of impurities on an atomic scale is essential to develop impurity-tolerant SOFCs with long-term durability. Here, we have studied the poisoning and degradation mechanisms of nickel anode by typical impurities, i.e. hydrogen sulfide, hydrogen chloride, etc., using density functional theory method.

Introduction

Solid oxide fuel cells (SOFCs) have long been proposed as the most efficient and versatile system for chemical to electrical energy conversion (1-5). One of the SOFC's advantages is the possibility of direct utilization of various types of fuels. Sulfur-containing impurities are present in practical SOFC fuels and are well known to lower the performance of metal catalyst such as nickel in the SOFC anode. Therefore, understanding the mechanism of sulfur poisoning is essential to develop sulfur-tolerant SOFCs with long durability. Density functional theory (DFT) is one of the useful methods to provide atomic-scale insight which is difficult to obtain from experimental approach. Some groups have reported the effect of sulfur adsorption on nickel surface using density functional theory (6-9). Wang et al. calculated the potential energy diagrams for hydrogen sulfide adsorption and dissociation on Ni(111) and (100) surfaces (6). Their results indicate that once hydrogen sulfide is supplied to the SOFC anode, hydrogen sulfide spontaneously dissociates and covers the nickel surface as a sulfur atom. Galea et al. showed adsorbed sulfur atom inhibits the dissociation of hydrogen molecules on Ni(111) surface (7). These studies provide a good support to understand the adsorption-type poisoning mechanism by sulfur-containing impurities. We also have studied the influence of sulfur on Ni-based SOFC anode and clarified the existence of subsurface atoms at higher hydrogen sulfide concentration (5), which is also suggested experimentally (10). However, regardless of the adsorbed or the subsurface sulfur atoms, the effects of sulfur on the long-term degradation and combined degradation of the SOFC anode are unclear. Here, we studied the influence of sulfur on the degradation mechanism

of the SOFC anode. We also studied the poisoning mechanism by other impurities using DFT.

Method

DFT calculations were performed using the CASTEP software package (11), with plane wave basis sets and pseudopotentials. All calculations were spin-polarized and conducted within the generalized gradient approximation (GGA) with the Perdew-Burke-Ernzerhof (PBE) exchange and correlation functionals (12). Each super cell consisted of three layers Ni slab with a vacuum layer of 8 Å. The Ni(111) or (100) surface is studied by using a 2x2 or 3x3 unit cell at the experimental lattice parameter (3.52 Å). The position of bottom of the Ni slab was fixed during the geometry optimization. An energy cutoff was set to 400 eV. The Brillouin zone was sampled by a 4x4x1 k-point Monkhorst-Pack grid. It should be noted that the convergence has been carefully checked changing the thickness of vacuum layer, the number of Ni layers, cutoff energy, and the number of sampling points. The increase in these parameters was found to change the binding energy of sulfur atom by less than 0.05 eV, and especially, the dependence on the size of vacuum layer and cutoff energy was less than 0.01 eV. In geometry optimizations, all adsorbate atoms and top and second layers of nickel atoms were relaxed. The size of super cell was fixed except for the test case checking the dependence of cell size. Energy and maximum force convergence thresholds were set to 1.0×10^{-5} eV/atom and 0.03 eV/Å, respectively.

Results and Discussion

Effect of Sulfur on Ni Sintering

In our previous study on sulfur poisoning (5), phase of subsurface sulfur appears at high concentration of hydrogen sulfide. We investigated its influence on the subsequent degradation by the sintering of Ni. Figure 1 shows the optimized surface structures with different sulfur coverage. θ_S is total sulfur coverage calculated considering both surface and subsurface sulfurs. We note that the structure with subsurface sulfur is less stable than one with surface sulfur for $\theta_S = 0.25$, thus the structure corresponds to either the minor structure under thermodynamic equilibrium at high temperature, the structure after desorption of surface sulfur or the structure where subsurface atom diffused from other sites such as surface step or triple-phase boundary. As shown in Fig. 1, existence of subsurface sulfur leads to the formation of Ni adatom, which is more mobile than the bulk Ni atoms.
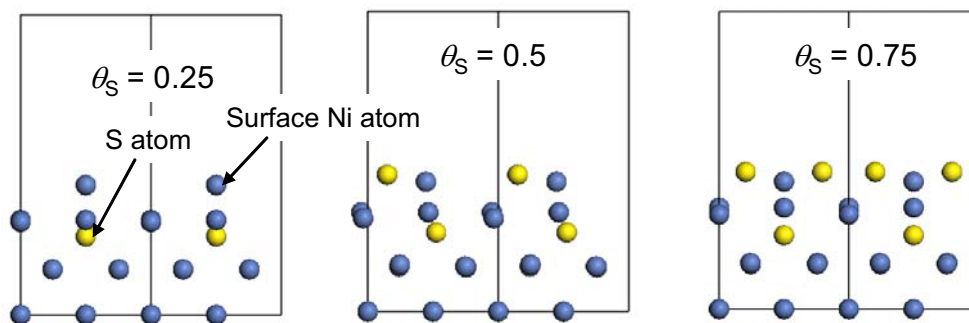

Figure 1. Structure change of Ni(100) surface induced by subsurface sulfur.

To see if the Ni adatom formation induced by the subsurface sulfur stays at a certain site or diffuses on the surface, we compared the energy of different surface states. Figure 2 shows the interim energy diagram for the selected states of Ni(100) surface after sulfur adsorption. States (ii) and (iv) correspond to structures of $\theta_S = 0.25$ and 0.75 in Fig. 1. Comparing the states (iv) and (v), it was clarified that the Ni adatom in state (iv) does not stay ontop of subsurface atom and diffuses away if there is vacant surface site nearby or further. Comparison of states (iv) and (ii) also suggests that once surface sulfur desorbs, for example due to gas phase concentration decrease, Ni adatom would diffuse away to free site though further investigation is necessary. From our interim results, we have obtained tentative insights on the influence of subsurface sulfur on the Ni sintering as followings:

1. Subsurface sulfur formation is associated with Ni adatom, which might accelerate Ni sintering by enhancing the formation of mobile Ni adatoms and the mobility of Ni adatoms

2. When surface sulfur concentration decreases by gas phase concentration change or operation temperature increase, isolated Ni adatom would be formed and it will become more mobile.

Above speculations should be pursued further by analyzing thoroughly the possible surface states and diffusion kinetics between those states in the subsequent study.
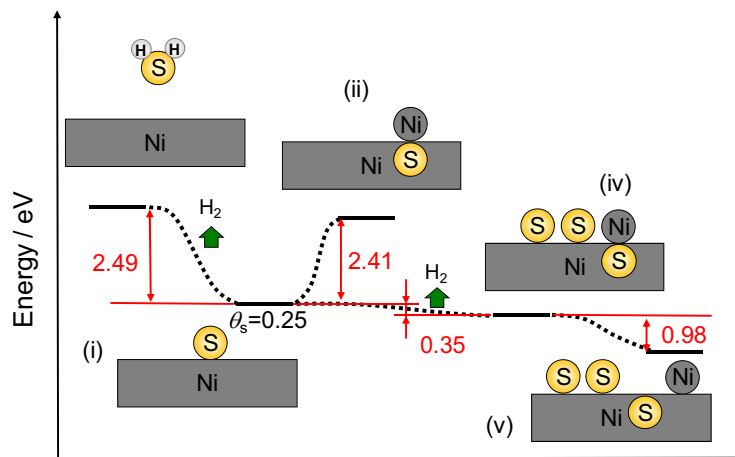

Figure 2. Energy diagram of different surface states after sulfur adsorption.

Effect of Sulfur on Carbon Deposition

Effect of sulfur on carbon deposition over nickel catalyst has been controversial for a long time. Some researchers reported that sulfur inhibits the rate of carbon deposition in steam methane reforming (13), while others reported sulfur promotes carbon deposition on nickel used for the SOFC anode with hydrocarbon fuels (14). We therefore investigated the interaction between carbon and sulfur atoms on nickel surface theoretically. Figure 3 shows the calculated binding energies of carbon atom on Ni(100) and (111) surfaces against surface sulfur coverage. We also show in Fig. 3 the binding energies of CS species, where carbon atom bonds with nickel surface and sulfur atom is over carbon atom, to see if the carbon and sulfur atoms stay isolated or chemically bond with each other on Ni surfaces. It was found that the carbon atom is relatively unstable on

Ni(111) surface and chemically bonds with sulfur atom to form CS species at higher sulfur coverage. On the contrary, carbon atom prefers to stay isolated on (100) surface even at high sulfur coverage. The results mean that the influence of sulfur on the adsorbed carbon depends on the surface orientation.
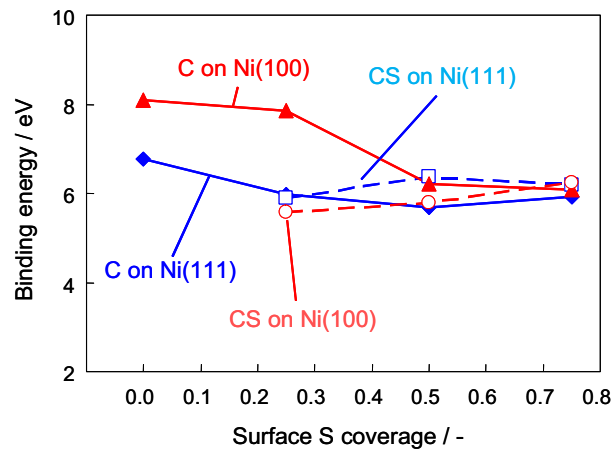

Figure 3. Binding energies of carbon and CS species on Ni surface with different sulfur coverage.

To see more in detail, we have analyzed the adsorption structure of carbon atoms focusing on Ni(100) surface. Figure 4 shows side views of adsorbed carbon on Ni(100) surface. When surface sulfur coverage is low, carbon atom is slightly above Ni top surface as shown in Fig. 2 ($\theta_S = 0$ and 0.25). On the contrary, carbon penetrates slightly into subsurface at higher sulfur coverage of 0.5 as shown in Fig. 3. To see the nature of this observation at the electronic level, we have analyzed the electronic density of the Ni surfaces. Figure 5 shows the electron density contour of Ni(100) surfaces with sulfur coverages of 0 and 0.5. Close comparison of side views of two cases, bottom of electron density contour for the top surface with 0.5 sulfur coverage is lower than that for the surface without sulfur. This means that the surface roughness increases by the sulfur adsorption. This can be interpreted to mean that the electron density around surface Ni atoms decreases due to higher electron affinity of adsorbed sulfur atoms.
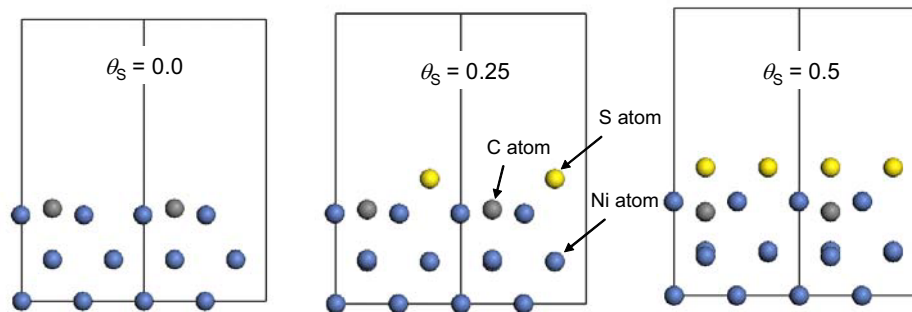

Figure 4. Change of carbon position on Ni surface by sulfur adsorption.

Here we summarize the insights obtained from the calculation results for higher sulfur coverage. The adsorbed carbon atom forms bond with surface sulfur atom on Ni(111), which may indicate that the carbon deposition may be suppressed because the C in CS species would not be a nucleation point resulting in the subsequent carbon deposition. On the contrary, carbon penetrates into subsurface at Ni(100) surface where density of surface atom is lower than that of Ni(111) surface. Because the subsurface carbon atom is

known to deactivate the Ni catalyst, sulfur may accelerate carbon deposition on Ni(100) surface.
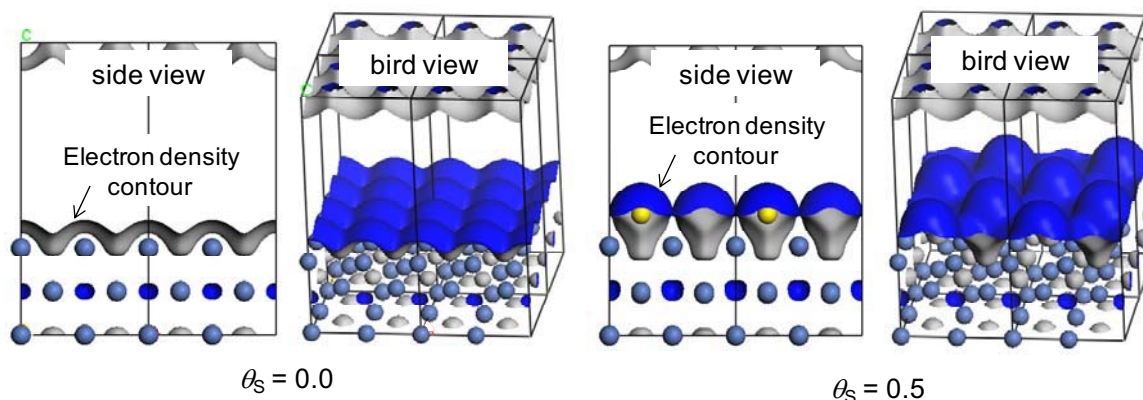

Figure 5. Electron density contours of Ni(100) surface with sulfur coverage of 0 and 0.5.

Poisoning by Halide Compounds

We then studied the adsorption of halogens to extend our analyses because it was reported that other impurities such as hydrogen chloride also have poisoning effect on nickel anode (15). Table 1 shows the calculated adsorption energies of hydrogen halides on various nickel surface sites. Results for hydrogen sulfide are also shown for reference. It was found that not only hydrogen chloride but also other hydrogen halides adsorb on nickel surface as halogen atom, which will reduce the active surface area available for fuel dissociation. However, those influences will be less significant compared with that by hydrogen sulfide, which shows stronger adsorption energy.

TABLE I. Calculated adsorption energies of impurities on various Ni surface sites (unit: eV).

Adsorbate / Adsorption Site	HF	HCl	HBr	HI	H_2S
Ni(111) fcc	-0.15	-1.10	-1.40	-1.77	-1.78
Ni(100) hollow	-0.20	-1.33	-1.67	-2.14	-2.49
Ni(100) bridge	-0.33	-1.16	-1.44	-1.80	-1.28
Ni(110) hollow	0.05	-0.97	-1.41	-1.97	-2.07
Ni(110) bridge	-0.60	-1.40	-1.63	-1.89	-1.19
Ni(211) step or edge	-0.74	-1.52	-1.75	-1.98	-2.26

Conclusions

In this study, we have investigated the influence of sulfur impurity on the sintering of Ni anode and carbon deposition. We have clarified that subsurface sulfur atom under high sulfur coverage leads to the formation of Ni adatom, which may accelerate the sintering of Ni anode. From the analyses for carbon deposition, different influences of sulfur were observed for Ni(111) and (100) surfaces with high sulfur coverage. C-S bond formation was observed on Ni(111) surface while subsurface carbon atom was observed for Ni(100) surface.

We extended our analyses to the poisoning effects by halogen impurities. It was found that hydrogen halide will adsorb on Ni surfaces, decreasing the surface active site

for electrochemical reaction. It was also found that the poisoning effects by halogen impurities are less significant compared to sulfur impurities.

Acknowledgments

References

1. M. Koyama, C. Wen, and K. Yamada, *J. Electrochem. Soc.*, **147**, 87 (2000).
2. H. Fukunaga, M. Koyama, N. Takahashi, C. Wen, and K. Yamada, *Solid State Ionics*, 132, 279 (2000).
3. M. Koyama, C. Wen, T. Masuyama, J. Otomo, H. Fukunaga, K. Yamada, K. Eguchi, and H. Takahashi, *J. Electrochem. Soc.*, **148**, A795 (2001).
4. T. Ota, M. Koyama, C. Wen, K. Yamada, and H. Takahashi, *J. Power Sources*, **118**, 430 (2003).
5. T. Ogura, T. Ishimoto, R. Nagumo, and M. Koyama, *Proc. 9th European SOFC Forum*, p. 7-128, (2010).
6. J. H. Wang and M. Liu, *Electrochem. Commun.*, **9**, 2212 (2007).
7. N. M. Galea, E. S. Kadantsev, and T. Ziegler, *J. Phys. Chem. C*, **111**, 14457 (2007).
8. E. J. Albenze and A. Shamsi, *Surf. Sci.*, **600**, 3202 (2006).
9. D. R. Alfonso, *Surf. Sci.*, **602**, 2758 (2008).
10. J. Hepola, J. McCarty, G. Krishnan, and V. Wong, *Appl. Catal. B*, **20**, 191 (1999).
11. S. J. Clark, M. D. Segall, C. J. Pickard, P. J. Hasnip, M. J. Probert, K. Refson, and M. C. Payne, *Z. Kristallogr.*, **220**, 567 (2005) and CASTEP official web site: http://www.castep.org/.
12. J. P. Perdew, K. Burke, and M. Ernzerhof, *Phys. Rev. Lett.*, **77**, 3865 (1996) and **78**, 1396 (1997).
13. J. R. Rostrup-Nielsen, *J. Catal.*, **85**, 31 (1984).
14. K. Sasaki, K. Haga, T. Yoshizumi, D. Minematsu, E. Yuki, R. Liu, C. Uryu, T. Oshima, T. Ogura, Y. Shiratori, K. Ito, M. Koyama, and K. Yokomoto, *J. Power Sources*, in press.
15. K. Haga, S. Adachi, Y. Shiratori, K. Ito, and K. Sasaki, *Solid State Ionics*, **179**, 1427 (2008).